Development of a platform for studying 3D astrocyte mechanobiology: compression of astrocytes in collagen gels

John J.E. Mulvihill,[1,2,a] Julia Raykin,[1,a] Eric J. Snider,[1] Lisa A. Schildmeyer,[1] Irsham Zaman,[1] Manu O. Platt,[1] Daniel J. Kelly,[2] and C. Ross Ethier[1,3*]

1. Wallace H. Coulter Department of Biomedical Engineering, Georgia Institute of Technology and Emory University, Atlanta, GA
2. Department of Mechanical and Manufacturing Engineering, School of Engineering, Trinity College Dublin, Dublin, Ireland
3. George W. Woodruff School of Mechanical Engineering, Georgia Institute of Technology, Atlanta, GA

* Corresponding author:
ross.ethier@bme.gatech.edu
315 Ferst Dr. NW, Atlanta, GA 30332

[a] Both of these authors contributed equally to this work

For submission to Annals of Biomedical Engineering

October 2017

Word count: 5976

Abstract

Glaucoma is a common optic neuropathy characterized by retinal ganglion cell death. Elevated intraocular pressure (IOP), a key risk factor for glaucoma, leads to significant biomechanical deformation of optic nerve head (ONH) cells and tissues. ONH astrocytes respond to this deformation by transforming to a reactive, proliferative phenotype, which has been implicated in the progression of glaucomatous vision loss. However, little is known about the mechanisms of this transformation. In this study, we developed a 3D collagen gel culture system to mimic features of ONH deformation due to elevated IOP. Compressive loading of astrocyte-seeded collagen gels led to cell alignment perpendicular to the direction of strain, and increased astrocyte activation, as assayed by GFAP, vimentin, and s100β levels, as well as MMP activity. This proof-of-concept study shows that this system has potential for studying mechanisms of astrocyte mechanobiology as related to the pathogenesis of glaucoma. Further work is needed to establish the possible interplay of mechanical stimulation, matrix properties, and hypoxia on the observed response of astrocytes.

Word count: 167

Key Terms: glaucoma; astrocyte mechanobiology; optic nerve head; 3D culture model; mechanical conditioning

Introduction

Glaucoma, an optic neuropathy characterized by patterns of visual field loss due to progressive loss of retinal ganglion cells (RGCs), is a leading cause of blindness worldwide.[49] While the exact mechanism of RGC damage is unknown, elevated intraocular pressure (IOP) is a known risk factor and a sustained reduction in IOP prevents the progression of vision loss in glaucoma patients,[2,18] indicating an important role for mechanobiology in this disease. RGC damage is thought to begin within the optic nerve head (ONH), which deforms in response to elevated IOP.[3,8,35] It is believed that ONH biomechanics, of which ONH deformation is one manifestation, significantly contributes to RGC loss in glaucoma.[20,23,27]

It has been hypothesized that astrocytes, the major glial cell type in the ONH, play an important role in the initiation of axonal damage.[19,23,25,30,44,48] Under healthy conditions, astrocytes maintain the extracellular matrix (ECM) within the ONH and provide trophic and metabolic support to RGC axons.[10,21] In response to pathological deformation, astrocytes transition from a quiescent phenotype to a more reactive, proliferative one.[19] A major hallmark of reactive astrocytes is the increased expression of glial fibrillary acidic protein (GFAP), vimentin, and s100β.[19,43] GFAP and vimentin help provide intracellular support and resistance to mechanical forces,[19] while s100β is expressed by proliferating astrocytes during neurite outgrowth.[26] Reactive astrocytes remodel the ONH via synthesis of various ECM proteins and matrix metalloproteinases (MMPs).[20,37] This tissue remodeling may contribute to RGC death by altering the normal biomechanical supportive functions of the ECM.[29,30,44]

Due to its anatomic features, the ONH experiences a variety of modes of biomechanical strain in response to IOP, with previous computational modeling studies indicating that compression is the major mode.[41] Therefore, it is of interest to understand how ONH astrocytes respond to compressive biomechanical strain. Thus far, the effects of mechanical strain on ONH astrocytes have only been studied in 2D under conditions of tension, not compression.[15,19,38] Further, 2D culture models do not accurately mimic the 3D physiological environment of the ONH, and in fact, have been shown to induce a reactive phenotype in cortical astrocytes.[14,34]

The purpose of this study was to develop a 3D in vitro system to study the effects of compressive biomechanical strain due to elevated IOP on ONH astrocyte mechanobiology. We demonstrate in this proof-of-concept study that a 3D culture system provides a good platform for studying astrocyte mechanoreactivity, and that cortical astrocytes respond to pathologic biomechanical stimulation by altering their orientation, expression of key reactivity markers, and protease activity.

Materials and Methods

Cell Sourcing

DI TNC1 cells (CRL 2005, ATCC), an immortalized cell line derived from primary cultures of type 1 astrocytes taken from brain diencephalon tissue of 1 day old rats,[36] were maintained at 37°C and 5% CO_2 in Dulbecco's Modified Eagle Medium (DMEM, Cellgro) supplemented with 10% fetal bovine serum (FBS, Hyclone, GE Healthcare) and 1x penicillin/streptomycin (Hyclone, GE Healthcare).

3D Collagen Gel Creation

3D collagen gel discs were cast at a collagen concentration of 2 mg mL^{-1} and $1x10^6$ cells mL^{-1} as previously described.[40] Briefly, lyophilized type I collagen derived from bovine skin (MP Biomedical) was dissolved in 0.02 N acetic acid to obtain a 2x collagen solution (4 mg mL^{-1}). DI TNC1 cells were mixed with 10x concentrated DMEM ($1/10^{th}$ of total final volume, Cellgro) and 2x collagen solution. 0.1 M sodium hydroxide was added immediately at $1/10^{th}$ the total volume as required to neutralize the solution. The 3D collagen gels were fabricated by adding 700 µL of the cell-laden collagen solution to a non-tissue culture treated 24-well plate (CytoOne), with a well diameter of 15.5 mm and gel height of 3.7 mm. The gels were allowed to polymerize for 15 minutes at 37°C, at which point 2 mL cell culture medium was added. After 24 hours, all gels were transferred to a 6-well plate for 7 days prior to mechanical stimulation, or placement in the static control chamber. Static control gels were placed in the indentations in the chamber floor (see below), and the plunger placed immediately above the gels to closely mimic the conditions of the stimulated gels and to prevent the gels from free-floating in the media. Fresh media was added to the gels every 2 days.

Mechanical Stimulation of Collagen Gels

To mimic the conditions of the ONH under elevated IOP, astrocyte-seeded collagen gel discs were cyclically compressed by 10% at 1 Hz for 24, 48, and 72 hours.[12,41] Our choice of 10% compression is broadly consistent with previous studies applying tensile strain to cultured ONH astrocytes in 2D,[16,38] and was originally motivated by previous finite element models that suggested that the ONH experiences compressive strains of 10% or more when IOP is 50 mmHg in humans.[41] While 50 mmHg is an admittedly high IOP, it was chosen here since it is seen in the clinic[24] and IOPs of above 50 mmHg are used in

acute studies of rat ocular hypertension.[28,47] This point is further discussed in detail in the Discussion section of the paper.

To apply the compressive mechanical load to the collagen gel discs, a custom-designed bioreactor system was developed (Figs. 1 and S1). The collagen gels (36 discs) were placed within an enclosed sterile chamber (thermoplastic polyester and transparent polycarbonate). Shallow indentations (6.5 mm in diameter and 0.1 mm in height) were made in the floor of chamber to prevent lateral motion of the discs during compression. 40 mL of media was added to the chamber, which was replenished each day. A linear actuator (Zaber Inc., NA08A30-T4), attached to a solid plunger (thermoplastic polyester) with a 5 mm clearance from the chamber wall, was set to cyclically compress (sinusoidally) the collagen gels by between 1 and 10% of the gel height. Static controls, not subject to compression, were cultured in an identical chamber for equivalent amounts of time. The actuator was positioned such that the platen was as close to the static control gels as possible without touching the gels. This approach allowed us to mimic the environment of the compressed gels as closely as possible, without the platen applying an unknown and uncontrolled load to the control gels. Thickness and diameter measurements were acquired using Vernier calipers. For 2D controls, cells were seeded at $2x10^4$ cells cm^{-2} on type I collagen-coated (10 µg cm^{-2}) silicone membranes for 72 hours.

FIGURE 1

Actin Labeling

Cell morphology was visualized via actin staining of whole mount collagen gels (Fig. 2a – top, left insert) and transverse sections (Fig. 2c – top, left insert) from the gels. For transverse sections, a 1 mm thick slice, perpendicular to the circular face, was extracted from the center of the whole mount gel using a scalpel. Gels were washed 3 times in PBS followed by fixation in 10% buffered formalin (Thermo Fisher Scientific) for 20 minutes. Following 3 further washes with PBS, cells in the samples were permeabilized by incubation with 0.1% (w/v) Triton X-100 for 15 minutes. Subsequently, the gels were incubated with Alexa Fluor 488 phalloidin (Thermo Fisher Scientific) at a 1:40 dilution for 1 hour.

FIGURE 2

Images from the whole mount gels and transverse sections were acquired via an inverted confocal microscope (LSM 700, Carl Zeiss). Z-stacks at increments of approximately 2.5 µm were taken through approximately 50 µm of the tissue starting from the top surface of the gel (arbitrarily chosen for the transverse sections). All images are presented as maximum intensity projections (MIPs) of z-stacks.

Astrocyte Alignment

Astrocyte orientation was assessed using the actin-labeled MIPs. To determine the isotropy of cellular alignment, images were acquired at each cardinal point on the 'circular face' of the gel (Fig. 2) as well as in the center. In these images the top of the gel was placed on the coverslip. In addition, transverse sections of the collagen gels were taken to better understand the alignment of the cells in 3D (Fig. 2c-d). Astrocyte alignment was quantified using the Fourier component analysis feature of the directionality plugin of FIJI

(http://fiji.sc/Fiji [in the public domain]). Histograms between −90° and 90° in 2° increments were generated (Fig. 2) and alignment indices were calculated to determine the degree of isotropy of the cells. An alignment index was computed as the fraction of the cells lying within 20° of the modal (most common) angle, normalized by the fraction of cells that would lie within that range in a uniformly random distribution.[31] Thus, an alignment index of 1 indicates random alignment, with higher values indicating less random alignment.

Protein Expression

Flow cytometry was used to quantify changes in protein expression in response to mechanical stimulation. To harvest the cells, the collagen gels were digested using collagenase type-2 (~400 units mL^{-1}, Worthington Biochemical, CLS-2), in live-cell imaging solution (Thermo Fisher Scientific) at 37°C for 20 minutes on an orbital rocker, which was followed by gentle trituration and filtration (35 µm nylon mesh filter; BD) of the collagenase solution to remove remaining large tissue debris. Next, the cells were centrifuged (300g for 5 minutes at 4°C) and resuspended in flow cytometry buffer (FCB, PBS containing 5% FBS and 0.02% (w/v) sodium azide) to wash the cells. Next, the cells were fixed with 2% (v/v) paraformaldehyde in PBS for 10 minutes, followed by two washes with FCB and 0.5% (w/v) saponin (Acros Organics) for permeabilization. Next, the cells were incubated at room temperature for 45 minutes with primary antibodies for GFAP, vimentin, and s100β diluted in FCB (see Table S1 for dilutions and antibody sources), supplemented with 0.5% (w/v) saponin for permeabilization. The cells were washed with FCB-0.5% saponin and stained with appropriate secondary antibodies (Table S1) in FCB-0.5% saponin. Dilutions and antibody information are provided in Table S1. Following an

178 additional wash step, the cells were resuspended in 300 µL FCB for analysis. Next, the
179 suspension was filtered one more time to remove any remaining debris. The 2D samples
180 were harvested from the silicone membranes using 0.05% trypsin and the samples were
181 prepared for flow cytometry as described above. Flow cytometry was carried out on a BD
182 Accuri C6 flow cytometer (35 µL min^{-1} flow rate, 100,000 cellular events per sample) and
183 median fluorescence intensity (MFI) values for each protein were determined with BD
184 Accuri C6 software. Compensation was carried out to correct for spectral overlap of the
185 fluorescent dyes via a compensation bead kit per manufacturer's instructions (Thermo
186 Fisher, A10497). To account for autofluorescence, MFI values of unstained controls were
187 subtracted from MFI values obtained for their respective stained sample. To account for
188 non-specific binding, flow cytometry samples were compared with respective isotype
189 controls (Table S1) to ensure increased MFI values were obtained in stained samples.

190 To confirm antibody specificity, Western blotting was carried out for each of the protein
191 markers used for flow cytometry per standard protocol. Briefly, collagen gels were
192 homogenized and protein concentrations were quantified via micro-BCA assay per
193 manufacturer's protocol (Thermo Scientific, Pierce Protein Research Products). For the
194 2D samples, cells were lysed and collected from the silicone membranes that they were
195 cultured on. Protein samples were denatured for 5 minutes at 95°C in Laemmli buffer
196 (Bio-Rad) and equal amounts of protein were loaded onto 8-16% polyacrylamide gels
197 (Bio-Rad) and sodium dodecyl sulfate-polyacrylamide gel electrophoresis (SDS-PAGE)
198 was carried out at 150 V for 45 minutes. Next, the resolved proteins were transferred to
199 polyvinyl difluoride (PVDF) membranes using a Trans-blot Turbo Transfer system (1.3 A
200 and 25 V for 7 minutes, Bio-Rad). Then the membranes were blocked with Odyssey

Blocking Buffer (LI-COR BioSciences). Due to the low molecular weight of s100β (21 kDa), it could not be successfully transferred from the polyacrylamide gels to the membranes in our system. Therefore, immunostaining was carried out directly on the polyacrylamide gels following SDS-PAGE. The polyacrylamide gels were placed in fixative solution (50% (v/v) isopropanol and 5% (v/v) acetic acid) for 1 hour. Both the membranes and the gels were probed with primary and secondary antibodies (Table S1) and imaged with an Amersham Imager 600 scanner (GE Healthcare).

MMP Activity

Gelatin zymography was used to quantify the MMP activity in the samples. Gels were homogenized using a post mounted homogenizer in lysis buffer (20 nM Tris-HCl at pH 7.5, 5 mM ethylene glycol-bis(β-aminoethyl ether)-N,N,N',N'-tetraacetic acid (EGTA), 150 mM NaCl, 20 mM β-glycerol-phosphate, 10 mM NaF, 1 mM sodium orthovanadate, 1% (v/v) Triton X-100, 0.1% (v/v) Tween-20) and 0.1 mM leupeptin, freshly added to stabilize enzymes during electrophoresis. 2D samples were prepared as described above. Gelatin zymography was carried out as previously described.[9,32] Briefly, protein concentrations were determined via micro-BCA assay. Next, equal amounts of protein in 5x non-reducing loading buffer (0.05% (w/v) bromophenol blue, 10% (w/v) SDS, 1.5 M Tris, 50% (v/v) glycerol) were resolved with 12.5% polyacrylamide gels (Protogel; National Diagnostics) containing 0.2% (w/v) gelatin at 4°C for 2 hours at 100 V in running buffer (25 mM Tris, 192 mM Glycine, 0.1% (w/v) SDS). Proteins were renatured in 65 mM Tris buffer, pH 7.4, with 20% (v/v) glycerol at room temperature for 30 minutes. Fresh buffer was added every 10 minutes, followed by incubation for 30 minutes in activity buffer (0.1 M sodium phosphate buffer, pH 6.0, 1 mM EDTA, and 2 mM DTT freshly added) at room

temperature. Then, the activity buffer was replaced with fresh activity buffer and allowed to incubate overnight at 37°C. Gels were then rinsed with deionized H_2O, incubated with Coomassie stain (10% (v/v) acetic acid, 25% (v/v) isopropanol, 4.5% (w/v) Coomassie Blue R-250) for 1 hour at room temperature and destained (10% (v/v) isopropanol and 10% (v/v) acetic acid) until gelatinolytic bands were evident, and imaged using the ImageQuant LAS 4000 (GE Healthcare). Densitometry analysis was performed in ImageQuant TL (GE Healthcare, v8.1).

Statistical Analysis

Statistical analysis was performed using Statistical Package for the Social Sciences (SPSS) Statistics software (IBM Inc.). The normality of all variables was examined using Shapiro-Wilk tests. Significant differences were identified between groups using two-way ANOVA analysis with post-hoc Sidak correction test. A p-value of less than 0.05 was considered statistically significant.

Results

Astrocyte Alignment

DI TNC1 rat cortical astrocytes were seeded into type I collagen gel discs and cultured statically for 7 days. The gels were cast at an initial diameter of 15.5 mm and height of 3.7 mm. After 7 days of static culture, during which time astrocytes proliferated in the gels, the cells contracted the gels to a diameter of 5.53 ± 0.02 mm (mean ± SEM, n=6) and a height of 2.32 ± 0.05 mm (mean ± SEM, n=6). The gels were then subjected to cyclic 10%

compression and compared to unloaded controls. No differences in volume were observed between the compressed and control gels.

We first investigated the changes in cellular orientation in response to cyclic mechanical compression of these collagen gel discs. The orientation of actin-labeled astrocytes was assessed in horizontal and transverse (Fig. 2 and S2) planes within collagen gel discs at 24, 48, and 72 hour time points. Random cell alignment was observed across all time points in the unloaded control gels (Figs. 2 and 3). Astrocytes within compressed gels demonstrated significantly increased alignment vs. unloaded gels in both the horizontal and transverse planes at each time point (Fig. 3), as well as a time-dependent increase in alignment over the 72 hour duration of the experiments. However, this alignment was spatially heterogeneous: cells near the periphery of the gel but not near the center showed alignment within a horizontal plane (Fig. 2). Conversely, cells near the center, but not near the periphery, showed alignment in a transverse plane. This was unexpected, as the theoretical strain distribution within the gel is spatially uniform (Fig. S3).

FIGURE 3

Astrocyte Activation

Three key markers associated with astrocyte activation, namely GFAP, vimentin, and s100β, were assayed via flow cytometry from astrocytes harvested from gels subjected to loading, and compared to levels from astrocytes from unloaded control gels. GFAP, vimentin, and s100β expression was significantly higher in astrocytes cultured in 2D than in astrocytes cultured statically (unloaded) in 3D collagen gels at 72 hours (Fig. 4). Expression of GFAP, vimentin, and s100β increased following mechanical stimulation as

compared to unloaded control collagen gels at each time point (Fig. 4). Western blots were performed on proteins isolated from compressed and control gels to confirm antibody specificity for each protein (Fig. S4).

FIGURE 4

Protease Activity

MMP-2 and MMP-9 activities were increased in mechanically stimulated astrocytes as compared to static control gels at each time point (Fig. 5). MMP-2 and MMP-9 activities were significantly higher in the compressed gels at 72 hours as compared to 24 and 48 hours. MMP activity in astrocytes grown in a 2D environment for 72 hours was significantly lower than that from cells in unloaded control gels.

FIGURE 5

DISCUSSION

Identifying mechanisms that lead to glaucomatous vision loss is of great importance for the development of clinical interventions. ONH astrocytes are believed to play a role in vision loss in glaucoma, yet their specific role in this process has not been fully elucidated. Because of the importance of biomechanics in glaucoma, techniques to understand how astrocytes respond to biomechanical strain are needed. As a complement to in vivo experiments, in vitro studies offer great potential in this regard; however, previous studies of ONH astrocyte mechanobiology have used monolayer-based approaches, which do not accurately represent the physiological environment of the ONH. Notably, monolayer

culture induces an artificially reactive phenotype in cultured astrocytes,[4,14] making it difficult to interpret the effect of biomechanical strain in such studies.

We present here a 3D culture system that has the potential to more accurately replicate key biomechanical features of the 3D ONH astrocyte environment by allowing the application of compressive biomechanical strains to the cells. Our data showed that astrocytes cultured in 3D collagen gels respond to mechanical stimulation through alterations in cell alignment. Specifically, in certain regions of the gel, the cells appeared to align perpendicular to the direction of the maximum principal strain (concentrically when viewed en face, horizontally when viewed in a transverse plane), whereas random alignment was observed in unloaded control gels (Figs. 2 and 3). This is consistent with studies performed on astrocytes in 2D, where the astrocytes aligned perpendicularly to the direction of strain.[6] We also observed a significant increase in cell alignment over the time course of mechanical stimulation, with the greatest increase occurring during the first 24 hours. Tehrani et al.,[47] observed a change in astrocyte orientation following an 8 hour increase in IOP in rats. Astrocyte orientation reverted to normal following IOP normalization, suggesting that astrocyte orientation changes dynamically in response to alterations in the tissue's local mechanical environment. Since this change in cell alignment occurred as early as 8 hours following a change in the homeostatic mechanical environment of the ONH, future studies should characterize astrocyte alignment at more frequent hourly intervals.

Interestingly, this cell alignment did not occur uniformly throughout the gel: in some regions, a random cell orientation persisted. It is unclear why this occurred. One possibility is that the gel did not deform homogenously when mechanically loaded.

Another possibility is that cell orientation could have been affected by local cellular density, leading to cell-mediated residual stresses due to unevenly generated contractile forces within the gels.[42] A final possibility for the observed cell alignment pattern could be due to non-uniform distribution of strain under cyclic compressive loading due to the poroelastic nature of the collagen gels coupled with the oscillatory compressive loading. Future studies should investigate these possibilities.

When analyzing the entire gel, we showed that mechanical stimulation increases astrocyte reactivity within collagen gels. Altered astrocyte reactivity is believed to be a significant component of glaucomatous ONH damage.[19,39] This altered reactivity was evidenced by increased expression of GFAP, vimentin, and s100β, and by increased activity of MMP-2 and MMP-9. MMP-2 and MMP-9 are known indicators of astrocyte activation and ECM remodeling, which could be an instigator of the changes in the biomechanical properties of the ONH during glaucoma progression.[23] Future work should characterize structural and compositional changes to the matrix in which the astrocytes are cultured.

Finally, we showed that this 3D culture platform induces less artificial astrocyte activation than cells cultured in a 2D monolayer. Notably, GFAP, vimentin, and s100β were expressed at lower levels in cells obtained from the 3D static controls than in cells cultured in a 2D monolayer (Fig. 4). However, MMP activity was significantly lower in astrocytes cultured in a 2D monolayer environment as compared to cells from the 3D unloaded control. This increased protease activity in a 3D environment compared to 2D has been observed in fibroblasts in previous studies,[22,46] and could be attributed to two possible factors: 1) in the 2D cultures, the MMPs could have been secreted into the cell culture

medium, since only cell lysates were assayed in our studies, and 2) proteolytic remodeling has been shown to be necessary for cell proliferation in 3D[7] and could lead to increased expression of MMPs in 3D as compared to 2D.

This study is subject to several limitations. First, the cell line used in this proof-of-concept study was an immortalized rat cell line obtained from cortical tissue rather than human ONH astrocytes. While these factors can influence astrocyte activation, our results are consistent with studies performed on ONH astrocytes in 2D and other types of astrocytes cultured in 3D. In addition, static controls are likely not ideal controls for the physiologic environment as ONH astrocytes are typically under mechanical loading. Future studies will incorporate a small strain (e.g. 3%) as the normal, healthy control[38] to compare to the effects of the pathological 10% strain on ONH astrocytes. In addition, an ideal in vitro model would impose a constant baseline strain, corresponding to a selected mean IOP, as well as a superimposed oscillatory strain, corresponding to the ocular pulse, typically 4 mmHg at 1 Hz. However, the precise magnitude of the appropriate cellular-level strains is surprisingly difficult to determine. Considering only the pulsatile component, interpolation of experimental data suggests that a 4 mmHg ocular pulse corresponds to a pulsatile peak macroscopic-level strain of c. 0.5% within the lamina cribrosa.[11] However, computational models suggest that macroscopic strain is significantly amplified at the cellular level in the lamina cribrosa, sometimes by a factor of 10 or more.[13] This would suggest that oscillatory strains of 5% or more are appropriate, which is broadly consistent with tensile oscillatory strains of 12% imposed in previous studies.[16,38] Therefore, we chose to simply impose a 10% compressive strain at 1 Hz. Future work should clearly include a range of strains and frequencies. Furthermore, while we did not observe any

355 change in volume between the compressed and control gels during compression, it is
356 possible that due to cellular compaction of the collagen matrix during the pre-compression
357 period, the choice of a collagen gel matrix in this study might not be optimal for tracking
358 the effects of compression on astrocyte activation. Further studies should utilize different
359 matrices that do not contract as readily, such as crosslinked collagen[33,45] or a collagen-
360 alginate mixture,[17] to more directly study the effects of strain on these cells. In addition, it
361 is possible that the observed differences between compressed and uncompressed gels
362 were due in part to nutrient transport limitations, including oxygen transport. To minimize
363 these effects the plunger face (platen) was positioned as close to the control gels as
364 possible. Further, as the platen was not in direct contact with the control gel's surface,
365 fluid motion over the gel surface was possible due to external factors such as incubator
366 vibrations. This could have resulted in different levels of hypoxia between the control and
367 experimental groups and it is therefore a possibility that the observed response is partially
368 due to hypoxic effects and not solely due to the applied mechanical deformation. Future
369 studies will include hypoxic assays to quantify oxygen levels and thus better understand
370 what effect transport limitations may have had in this system.

371 Moreover, while a cell-seeded disk was a necessary starting point in this preliminary
372 study, it is only a simplified representation of the ECM in the ONH. Further, it is possible
373 that a 10% compression of these gels does not lead to a 10% compression of the cells
374 themselves.[5] Characterization of the strain field throughout the gel/cells was not possible
375 with the current design of the system due to the use of non-transparent materials that
376 prevented optical interrogation of the gels. In the future, we plan to use a transparent

base in the bioreactor system that will allow for imaging and characterization of the strain field via digital image correlation methods.

Importantly, due to the limitations of in vitro studies it is not possible to completely mimic the in vivo environment of the ONH. For instance, surrounding tissues such as the sclera and choroid play an important role in the deformation of the ONH and help to determine the complex deformations of the ONH in vivo. Furthermore, the collagen gel does not truly mimic the structure and composition of the lamina cribrosa, which contains a dense intricate dispersion of various types of collagens (I, III, IV, V, and VI) as well as elastin,[1] and therefore the load applied to the cells in a less dense collagen gel does not completely mimic the load on the cells in the ONH in vivo. Future studies will utilize more dense scaffolds (e.g. crosslinked collagen or a collagen-alginate mixture) to develop a system that more accurately resembles the material properties of the ONH. In addition, other cell types from the ONH and these surrounding tissues should be incorporated into this system in the future, as they might affect the astrocyte response to deformation. Finally, while the main mode of deformation in the lamina cribrosa is compression, the deformations in vivo are complex and thus this system does not completely mimic the in vivo mechanical environment of the ONH. Future studies will include the effects of more complex loading conditions on astrocytes to more accurately characterize the effects of in vivo mechanical loading on the astrocytes of the ONH.

In conclusion, we have developed a 3D system to study the effects of IOP-induced deformation on astrocytes. This is an important first step in the development of a physiologically relevant in vitro platform to study ONH astrocyte mechanobiology. Further

analysis of astrocytic response to deformation will advance the understanding of glaucoma and enable the development of future therapeutics and interventions.

ACKNOWLEDGEMENTS

This work was supported by the Georgia Research Alliance, the Irish Research Council through the ELEVATE: Irish Research Council International Career Development Fellowship – co-funded by Marie Curie Actions, the National Space Biomedical Research Institute through NCC 9-58, and the National Science Foundation Graduate Research Fellowship under Grant No. DGE-1148903.

REFERENCES

1. Albon, J., W. S. Karwatowski, N. Avery, D. L. Easty, and V. C. Duance. Changes in the collagenous matrix of the aging human lamina cribrosa. *Br J Ophthalmol* 79:368–375, 1995.

2. Anderson, D. R. Collaborative normal tension glaucoma study. *Curr Opin Ophthalmol* 14:86–90, 2003.

3. Anderson, D. R., and A. Hendrickson. Effect of Intraocular Pressure on Rapid Axoplasmic Transport in Monkey Optic Nerve. *Invest Ophthalmol Vis Sci* , 1974.

4. Balasubramanian, S., J. A. Packard, J. B. Leach, and E. M. Powell. Three-Dimensional Environment Sustains Morphological Heterogeneity and Promotes Phenotypic Progression During Astrocyte Development. *Tissue Eng Part A* 22:885–898, 2016.

5. Bell, B. J., E. Nauman, and S. L. Voytik-Harbin. Multiscale strain analysis of tissue equivalents using a custom-designed biaxial testing device. *Biophys J* 102:1303–1312, 2012.

6. Biran, R., M. D. Noble, and P. A. Tresco. Directed nerve outgrowth is enhanced by engineered glial substrates. *Exp Neurol* 184:141–152, 2003.

7. Bott, K., Z. Upton, K. Schrobback, M. Ehrbar, J. A. Hubbell, M. P. Lutolf, and S. C. Rizzi. The effect of matrix characteristics on fibroblast proliferation in 3D gels. *Biomaterials* 31:8454–8464, 2010.

8. Burgoyne, C. F., J. C. Downs, A. J. Bellezza, J.-K. F. Suh, and R. T. Hart. The optic nerve head as a biomechanical structure: a new paradigm for understanding the role of IOP-related stress and strain in the pathophysiology of glaucomatous optic nerve head damage. *Prog Retin Eye Res* 24:39–73, 2005.

9. Chen, B., and M. O. Platt. Multiplex zymography captures stage-specific activity profiles of cathepsins K, L, and S in human breast, lung, and cervical cancer. *J Transl Med* 9:109, 2011.

10. Chong, R. S., and K. R. Martin. Glial cell interactions and glaucoma. *Curr Opin Ophthalmol* 26:73–77, 2015.

11. Coudrillier, B., D. Geraldes, N. Vo, R. Atwood, C. Reinhard, I. Campbell, Y. Raji, J. Albon, R. Abel, and R. Ethier. Phase-contrast Micro-computed Tomography Measurements of the Intraocular Pressure-induced Deformation of the Porcine Lamina Cribrosa. *IEEE Trans Med Imaging* 35:988–999, 2015.

12. Downs, J. C., C. F. Burgoyne, W. P. Seigfreid, J. F. Reynaud, N. G. Strouthidis, and V. Sallee. 24-hour IOP telemetry in the nonhuman primate: implant system performance and initial characterization of IOP at multiple timescales. *Invest Ophthalmol Vis Sci* 52:7365–7375, 2011.

13. Downs, J. C., M. D. Roberts, and C. F. Burgoyne. Mechanical environment of the optic nerve head in glaucoma. *Optom Vis Sci* 85:425–435, 2008.

14. East, E., J. P. Golding, and J. B. Phillips. A versatile 3D culture model facilitates monitoring of astrocytes undergoing reactive gliosis. *J Tissue Eng Regen Med* 3:634–646, 2009.

15. Ellis, E. F., J. S. McKinney, K. A. Willoughby, S. Liang, and J. T. Povlishock. A new model for rapid stretch-induced injury of cells in culture: characterization of the model using astrocytes. *J Neurotrauma* 12:325–339, 1995.

16. Exler, R. E., X. Guo, D. Chan, I. Livne-Bar, N. Vicic, J. G. Flanagan, and J. M. Sivak. Biomechanical insult switches PEA-15 activity to uncouple its anti-apoptotic function and promote erk mediated tissue remodeling. *Exp Cell Res* 340:283–294, 2016.

17. Gillette, B. M., J. A. Jensen, M. Wang, J. Tchao, and S. K. Sia. Dynamic hydrogels: switching of 3D microenvironments using two-component naturally derived extracellular matrices. *Adv Mater Weinheim* 22:686–691, 2010.

18. Heijl, A., M. C. Leske, B. Bengtsson, L. Hyman, B. Bengtsson, M. Hussein, and Early Manifest Glaucoma Trial Group. Reduction of intraocular pressure and

glaucoma progression: results from the Early Manifest Glaucoma Trial. *Arch Ophthalmol* 120:1268–1279, 2002.

19. Hernandez, M. R. The optic nerve head in glaucoma: role of astrocytes in tissue remodeling. *Prog Retin Eye Res* 19:297–321, 2000.

20. Hernandez, M. R., H. Miao, and T. Lukas. Astrocytes in glaucomatous optic neuropathy. In: Glaucoma: An Open Window to Neurodegeneration and Neuroprotection. Elsevier, 2008, pp. 353–373.doi:10.1016/S0079-6123(08)01125-4

21. De Hoz, R., B. Rojas, A. I. Ramírez, J. J. Salazar, B. I. Gallego, A. Triviño, and J. M. Ramírez. Retinal macroglial responses in health and disease. *BioMed research international* 2016:2954721, 2016.

22. Jaworski, J., and C. M. Klapperich. Fibroblast remodeling activity at two- and three-dimensional collagen-glycosaminoglycan interfaces. *Biomaterials* 27:4212–4220, 2006.

23. Johnson, E. C., and J. C. Morrison. Friend or foe? Resolving the impact of glial responses in glaucoma. *J Glaucoma* 18:341–353, 2009.

24. Lam, D. S. C., J. K. H. Chua, C. C. Y. Tham, and J. S. M. Lai. Efficacy and safety of immediate anterior chamber paracentesis in the treatment of acute primary angle-closure glaucoma: a pilot study. *Ophthalmology* 109:64–70, 2002.

25. Lye-Barthel, M., D. Sun, and T. C. Jakobs. Morphology of astrocytes in a glaucomatous optic nerve. *Invest Ophthalmol Vis Sci* 54:909–917, 2013.

26. Marshak, D. R. S100 beta as a neurotrophic factor. *Prog Brain Res* 86:169–181, 1990.

27. Morgan, J. E. Optic nerve head structure in glaucoma: astrocytes as mediators of axonal damage. *Eye (Lond)* 14 (Pt 3B):437–444, 2000.

28. Morrison, J. C., W. O. Cepurna, S. Tehrani, T. E. Choe, H. Jayaram, D. C. Lozano, B. Fortune, and E. C. Johnson. A period of controlled elevation of IOP (CEI) produces the specific gene expression responses and focal injury pattern of experimental rat glaucoma. *Invest Ophthalmol Vis Sci* 57:6700–6711, 2016.

29. Munemasa, Y., and Y. Kitaoka. Molecular mechanisms of retinal ganglion cell degeneration in glaucoma and future prospects for cell body and axonal protection. *Front Cell Neurosci* 6:60, 2012.

30. Neufeld, A. H., and B. Liu. Glaucomatous optic neuropathy: when glia misbehave. *Neuroscientist* 9:485–495, 2003.

494 31. Ng, C. P., B. Hinz, and M. A. Swartz. Interstitial fluid flow induces myofibroblast
495 differentiation and collagen alignment in vitro. *J Cell Sci* 118:4731–4739, 2005.

496 32. Nguyen, A. H., Y. Wang, D. E. White, M. O. Platt, and T. C. McDevitt. MMP-
497 mediated mesenchymal morphogenesis of pluripotent stem cell aggregates
498 stimulated by gelatin methacrylate microparticle incorporation. *Biomaterials* 76:66–
499 75, 2016.

500 33. Orban, J. M., L. B. Wilson, J. A. Kofroth, M. S. El-Kurdi, T. M. Maul, and D. A. Vorp.
501 Crosslinking of collagen gels by transglutaminase. *J Biomed Mater Res A* 68:756–
502 762, 2004.

503 34. Placone, A. L., P. M. McGuiggan, D. E. Bergles, H. Guerrero-Cazares, A.
504 Quiñones-Hinojosa, and P. C. Searson. Human astrocytes develop physiological
505 morphology and remain quiescent in a novel 3D matrix. *Biomaterials* 42:134–143,
506 2015.

507 35. Quigley, H. A., and E. M. Addicks. Chronic experimental glaucoma in primates. II.
508 Effect of extended intraocular pressure elevation on optic nerve head and axonal
509 transport. *Invest Ophthalmol Vis Sci* 19:137–152, 1980.

510 36. Radany, E. H., M. Brenner, F. Besnard, V. Bigornia, J. M. Bishop, and C. F.
511 Deschepper. Directed establishment of rat brain cell lines with the phenotypic
512 characteristics of type 1 astrocytes. *Proc Natl Acad Sci U S A* 89:6467–6471, 1992.

513 37. Ridet, J. L., S. K. Malhotra, A. Privat, and F. H. Gage. Reactive astrocytes: cellular
514 and molecular cues to biological function. *Trends Neurosci* 20:570–577, 1997.

515 38. Rogers, R. S., M. Dharsee, S. Ackloo, J. M. Sivak, and J. G. Flanagan. Proteomics
516 analyses of human optic nerve head astrocytes following biomechanical strain. *Mol*
517 *Cell Proteomics* 11:M111.012302, 2012.

518 39. Schneider, M., and R. Fuchshofer. The role of astrocytes in optic nerve head
519 fibrosis in glaucoma. *Exp Eye Res* 142:49–55, 2016.

520 40. Seliktar, D., R. A. Black, R. P. Vito, and R. M. Nerem. Dynamic mechanical
521 conditioning of collagen-gel blood vessel constructs induces remodeling in vitro.
522 *Ann Biomed Eng* 28:351–362, 2000.

523 41. Sigal, I. A., J. G. Flanagan, I. Tertinegg, and C. R. Ethier. Predicted extension,
524 compression and shearing of optic nerve head tissues. *Exp Eye Res* 85:312–322,
525 2007.

42. Simon, D. D., C. O. Horgan, and J. D. Humphrey. Mechanical restrictions on biological responses by adherent cells within collagen gels. *J Mech Behav Biomed Mater* 14:216–226, 2012.

43. Sofroniew, M. V., and H. V. Vinters. Astrocytes: biology and pathology. *Acta Neuropathol* 119:7–35, 2010.

44. Son, J. L., I. Soto, E. Oglesby, T. Lopez-Roca, M. E. Pease, H. A. Quigley, and N. Marsh-Armstrong. Glaucomatous optic nerve injury involves early astrocyte reactivity and late oligodendrocyte loss. *Glia* 58:780–789, 2010.

45. Sundararaghavan, H. G., G. A. Monteiro, N. A. Lapin, Y. J. Chabal, J. R. Miksan, and D. I. Shreiber. Genipin-induced changes in collagen gels: correlation of mechanical properties to fluorescence. *J Biomed Mater Res A* 87:308–320, 2008.

46. Sung, K. E., X. Su, E. Berthier, C. Pehlke, A. Friedl, and D. J. Beebe. Understanding the impact of 2D and 3D fibroblast cultures on in vitro breast cancer models. *PLoS ONE* 8:e76373, 2013.

47. Tehrani, S., L. Davis, W. O. Cepurna, T. E. Choe, D. C. Lozano, A. Monfared, L. Cooper, J. Cheng, E. C. Johnson, and J. C. Morrison. Astrocyte Structural and Molecular Response to Elevated Intraocular Pressure Occurs Rapidly and Precedes Axonal Tubulin Rearrangement within the Optic Nerve Head in a Rat Model. *PLoS ONE* 11:e0167364, 2016.

48. Tehrani, S., E. C. Johnson, W. O. Cepurna, and J. C. Morrison. Astrocyte processes label for filamentous actin and reorient early within the optic nerve head in a rat glaucoma model. *Invest Ophthalmol Vis Sci* 55:6945–6952, 2014.

49. Tham, Y.-C., X. Li, T. Y. Wong, H. A. Quigley, T. Aung, and C.-Y. Cheng. Global prevalence of glaucoma and projections of glaucoma burden through 2040: a systematic review and meta-analysis. *Ophthalmology* 121:2081–2090, 2014.

FIGURES

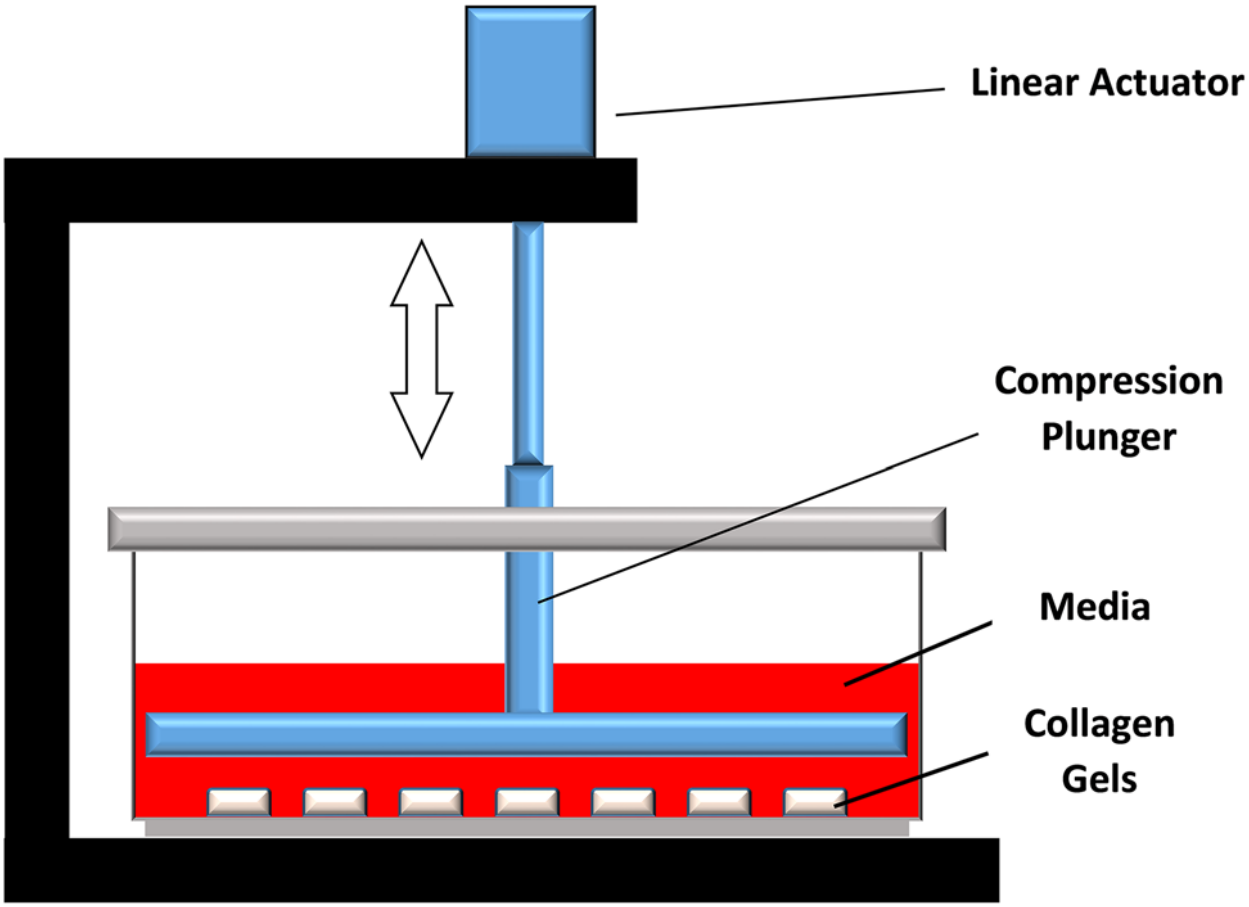

FIGURE 1: Bioreactor schematic. Cyclic compressive load was applied to multiple collagen gels using a linear actuator and plunger located in an enclosed, sterile culture chamber.

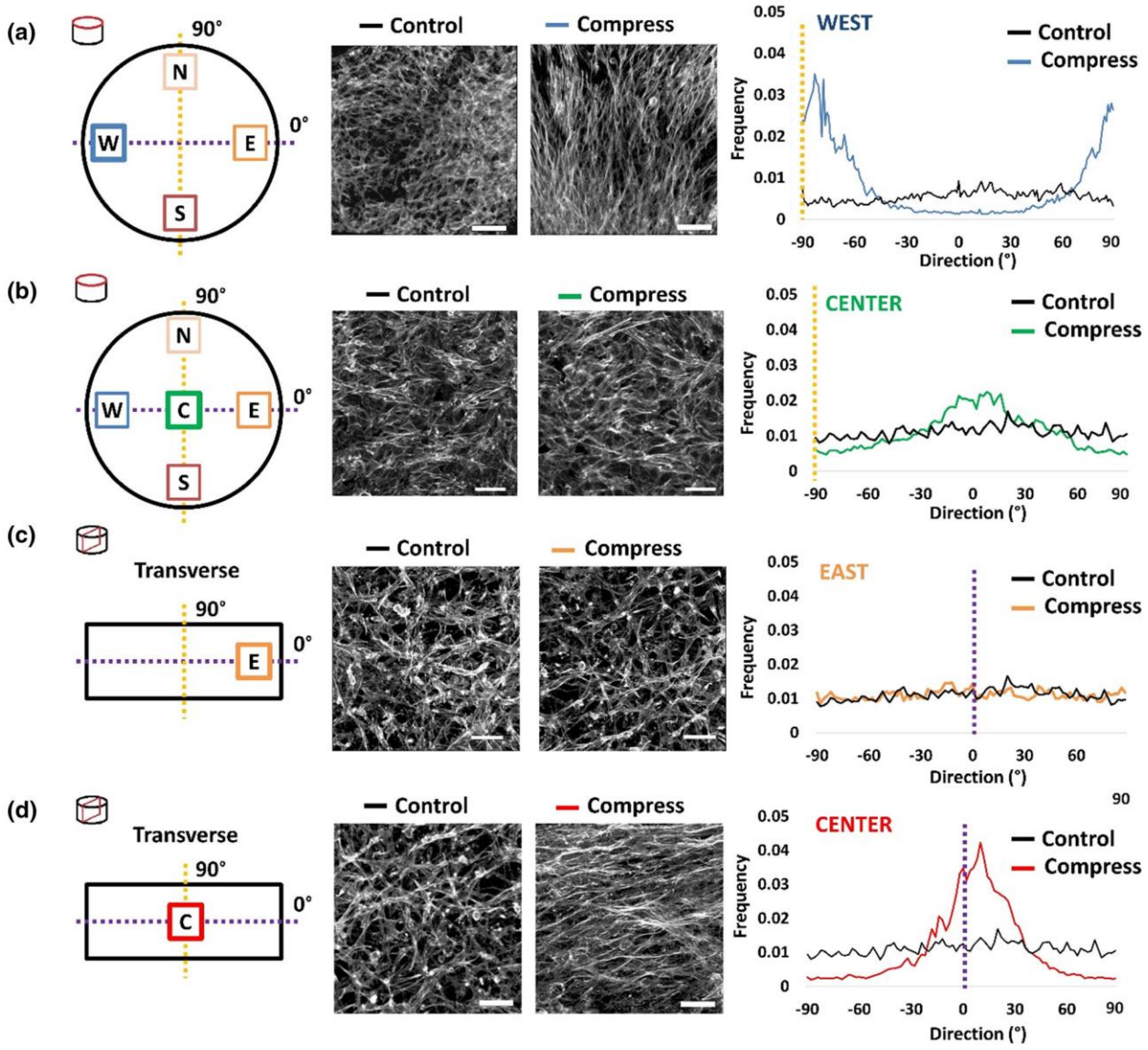

FIGURE 2: Effects of mechanical loading on alignment of astrocytes seeded within collagen type I discs. Representative maximum intensity projections (MIP) of actin labeled astrocytes in unloaded control and compressed gels at 24 hours taken at various locations of the gel, namely the (A) west and (B) center locations of a horizontally oriented plane, and in the (C) east and (D) center locations of a transverse plane. Left columns show the locations in the gel where the images in the middle column were taken and the right column shows histograms of the cell orientations of these images. The images in (A)

566 are representative of the four cardinal directions at the periphery of the gels. Histograms
567 were generated from 320x320 µm MIPs. All MIPs were acquired from z-stacks taken at
568 2.5 µm increments consisting of 20 total images starting from the top of the gel for images
569 acquired in the horizontally oriented plane and arbitrarily chosen for images acquired in
570 the transverse plane. Purple dashes indicate horizontal astrocyte alignment, while yellow
571 dashes indicate vertical alignment. Scale bars: 50 µm.

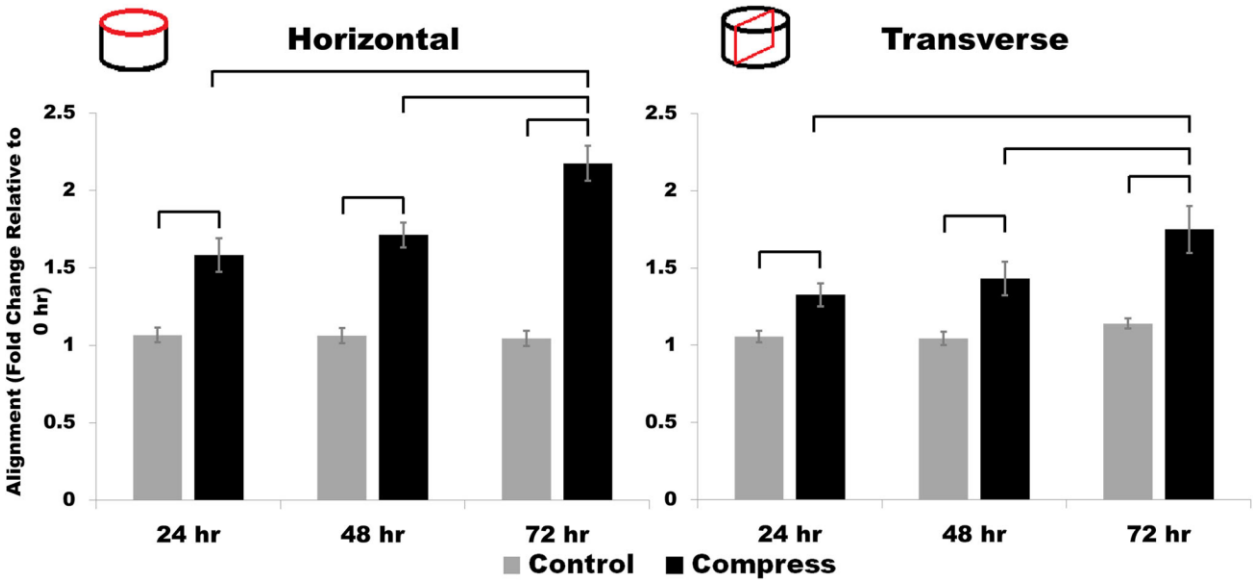

572

573 **FIGUREE 3. Astrocyte alignment in 3D collagen gels.** Alignment indices (see text) for
574 control and compressed collagen type I gel discs normalized to 0 hour static controls at
575 24, 48, and 72 hour time points. “Horizontal” refers to cell alignment averaged from 4
576 regions near the gel periphery representing all 4 cardinal directions (Fig. 1A), as viewed
577 in the imaging plane indicated at top left. Similarly, “transverse” refers to cell alignment
578 within a single central region, as viewed in the imaging plane at top left. These are regions
579 where cell alignment was observed. Brackets indicate $p \leq 0.05$; error bars indicate
580 standard error of the mean of n=4.

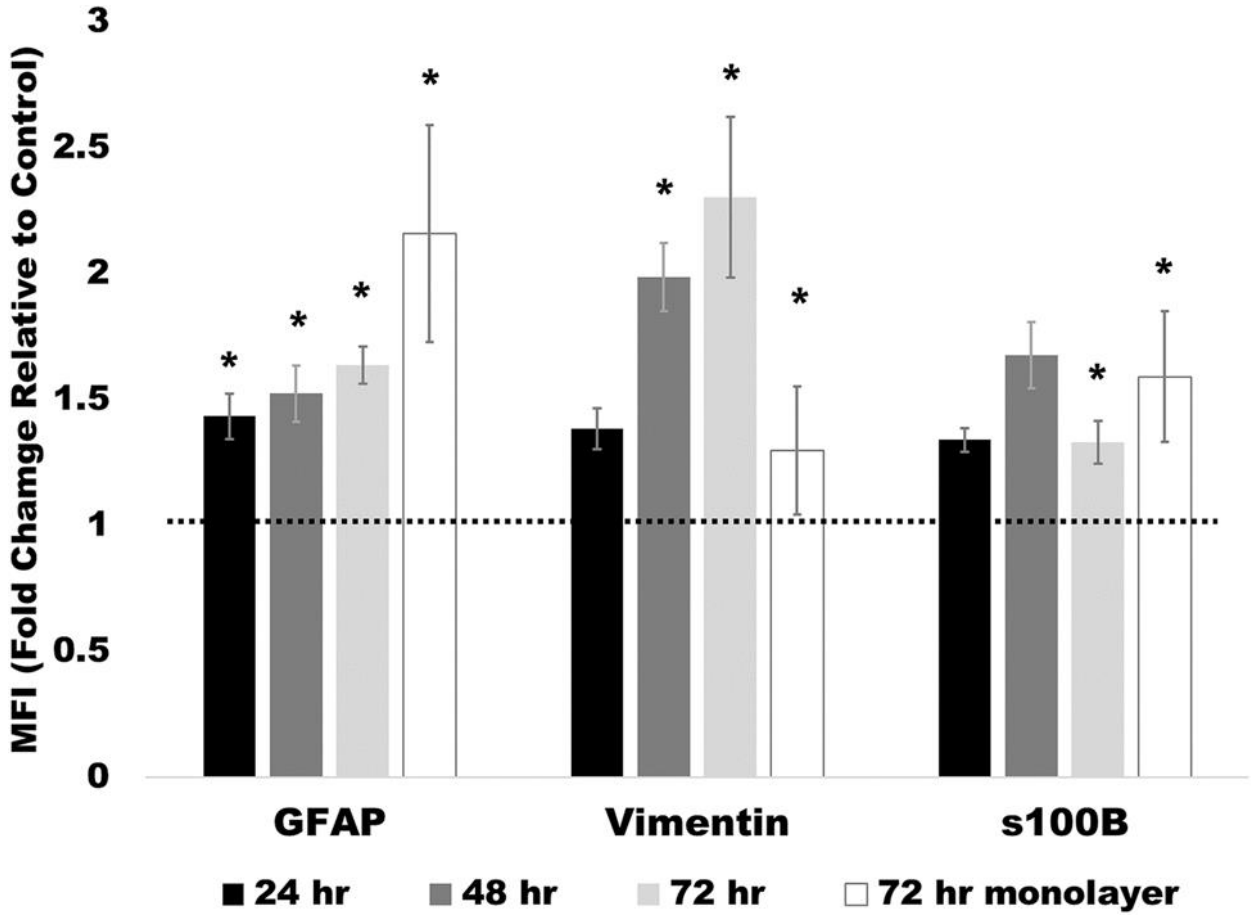

FIGURE 4: Expression of GFAP, vimentin, and s100β from astrocytes in 3D collagen type I gels and from 72 hour monolayer controls. Normalized median fluorescence intensity (MFI) of GFAP, vimentin, and s100β obtained via flow cytometry of astrocytes isolated from static and compressed and control collagen gels at each time point as well as 72 hour monolayer static controls. Note that since flow cytometry was performed on freshly fixed cells it was not possible to normalize to 0 hour data in this case. Therefore, each condition was normalized by its respective unloaded control. Data from 2D culture was normalized to the 72 hour unloaded 3D gel control. * indicates $p \leq 0.05$ comparing MFI values of compressed gels to respective time controls, error bars indicate standard error of the mean of n=4.

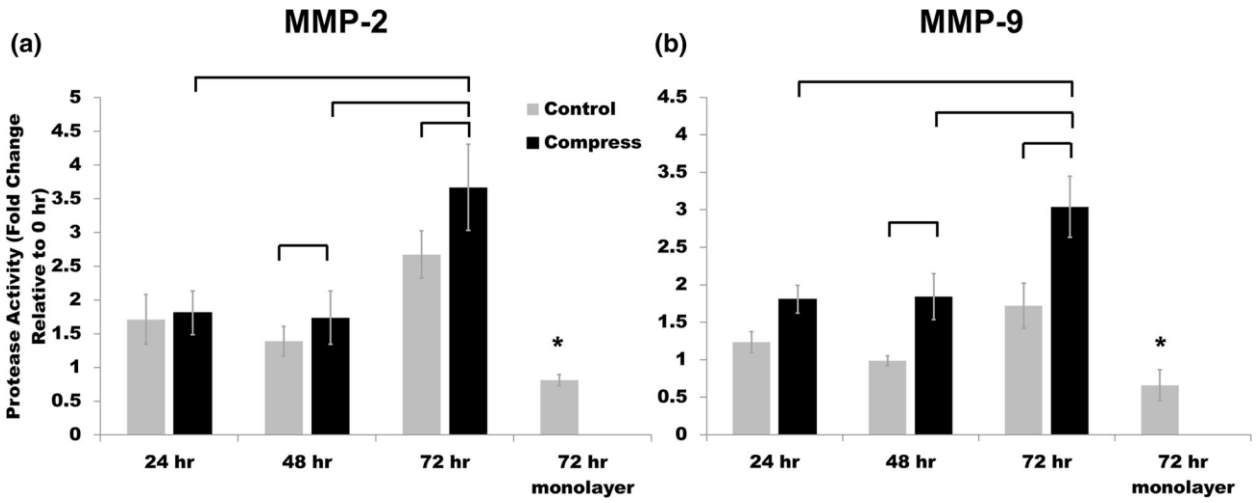

592

593 **FIGURE 5: Protease activity from astrocytes in 3D collagen type I gels and from 72**
594 **hour monolayer controls as determined by gelatin zymography.** (A) MMP-2 and (B)
595 MMP-9 activities. All values are normalized to 0 hour static control. Brackets indicate
596 $p \leq 0.05$, * indicates $p \leq 0.05$ for 72 hour monolayer compared to 72 hour static control, error
597 bars indicate standard error of the mean of n=6.

598